BREACH EROSION IN SAND-DIKES

by

Paul J. Visser [1]

ABSTRACT

The process of breach erosion in sand-dikes is described. This process consists of five stages. For the final two stages three breach types are distinguished, depending on the erodibility of the base of the dike, the presence (or absence) of a solid toe construction on the outer slope and the presence and erodibility of a high foreland. A brief outline of a mathematical model based on the five-step breach growth process is presented. The validation of the model against the data of a field experiment shows good agreement.

1. INTRODUCTION

The Technical Advisory Committee on Water Defences (TAW) in the Netherlands has decided to substitute an inundation risk approach for the present design method for dikes based on an exceedance frequency of the water level. In this new method safety levels will be expressed in terms of risks. A risk-norm means that the inundation chance is combined with the consequences of flooding (deaths, loss of property and revenues, etc.), see Kraak et al. (1995). In order to determine the consequences of inundation, it is necessary to predict both the rate and speed of polder flooding. These are especially governed by the flow rate through the breach in the dike, which in its turn largely depends on the process of breach growth.

The aim of the investigation is a mathematical model that predicts the breach growth and the discharge through the breach in case of a dike-burst as function of relevant parameters as the cross-section of the dike (height, width, slope angles), the structure of the dike (dike material, revetments, foundation), polder area and the hydraulic conditions (water level against the dike, wave load). It is assumed that the dike was constructed with sand and that, after the formation of an initial breach at

[1] Delft University of Technology, Department of Civil Engineering, P.O. Box 5048, 2600 GA Delft, The Netherlands

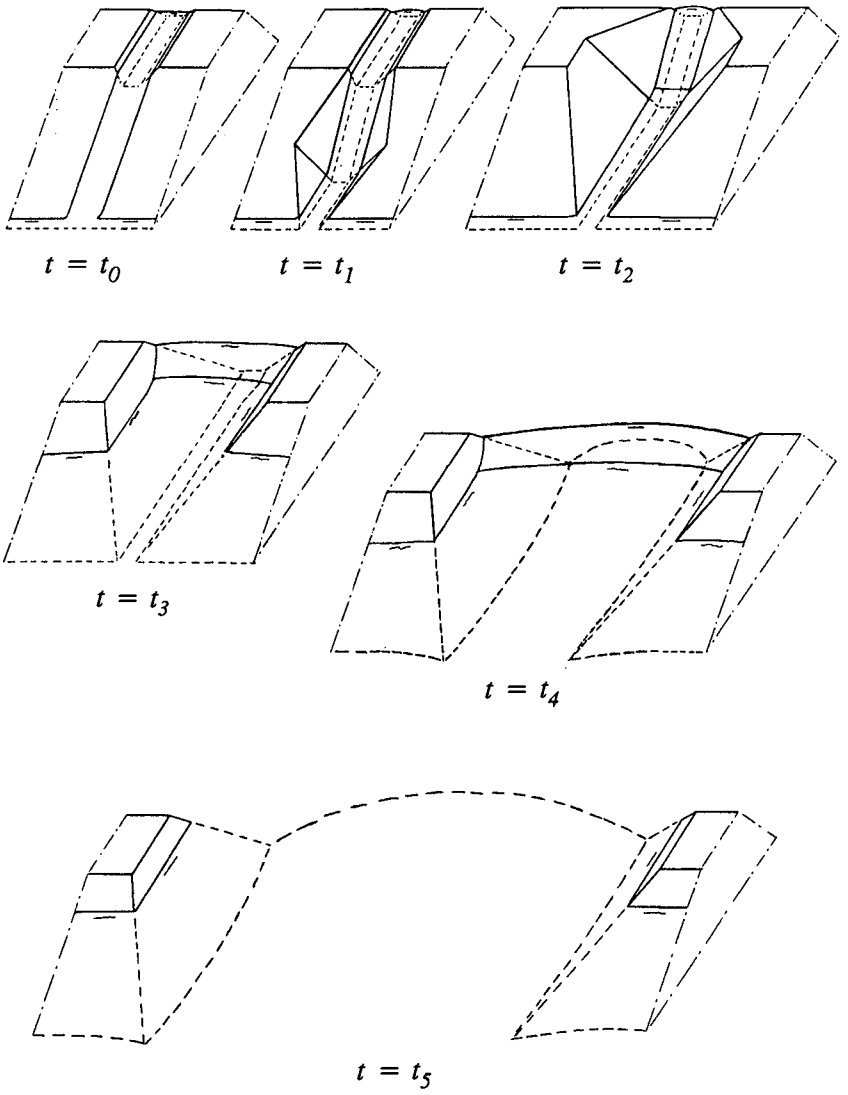

Figure 1 Schematic illustration of breach growth in a sand-dike.

the top of the dike, the clay-layers on the slopes do not decelerate the erosion process.

The first versions of the model (see Visser, 1995a) have been focused on the first three stages of the breach erosion process. The present model version includes also the final two stages of the dike breaching process. Also some improvements related to the physics of the erosion process have been implemented into the model.

2. BREACH EROSION PROCESS

It is assumed that the breach erosion starts (at $t = t_0$) with the flow of water through a small initial breach at the top of the sand-dike with a trapezoidal cross-section. Generally five stages can be distinguished in the process of breach erosion (see Figure 1). These five stages are:

- Stage I: steepening of the slope angle β of the channel in the inner dike slope from an initial value β_0 at $t = t_0$ up to a critical value β_1 at $t = t_1$.
- Stage II: retrograde erosion of the inner dike slope at constant angle β_1 for $t_1 < t \leq t_2$, yielding a decrease of the width of the crest of the dike in the breach; this stage ends at t_2 when the crest vanishes and the breach inflow starts to increase.
- Stage III: lowering of the top of the dike in the breach, with constant angle of the breach side-slopes and equal to the critical value γ_1, resulting in an increase of the width of the breach for $t_2 < t \leq t_3$. At $t = t_3$ the dike in the breach is completely washed out down to the base of the dike at polder level.
- Stage IV: critical flow stage, in which the breach flow is virtually critical throughout the breach for $t_3 < t \leq t_4$, and the breach continues to grow mainly laterally. The side-slope angles remain at the critical value γ_1. The breach growth in vertical direction depends in this stage on the erodibility of the base the dike. At t_4 the flow through the breach changes from critical ($Fr = 1$ in Stage IV to subcritical ($Fr < 1$ for $t > t_4$).
- Stage V: subcritical flow stage, in which the breach continues to grow, mainly laterally due to the subcritical flow in the breach for $t_4 < t \leq t_5$. The side-slope angles remain at the critical value γ_1. At t_5 the flow velocities in the breach become so small (incipient motion) that the breach erosion stops. The flow through the breach continues and stops when at t_6 the water level in the polder has equalled the outside water level.

In Stages I, II and III the initial breach cuts itself into the dike. Most of the discharge through the breach takes place in the Stages IV and V. At the end of Stage IV backwater starts to effect the flow through the breach. In case of a relatively tiny polder with a very small storage capacity, the downstream submergence may start earlier. In theory this may occur in each of the Stages I, II and III. In practice, however, it will take place in Stage III, since the total flow through the breach is too small in Stages I and II to allow downstream submergence. Hence, in case of a relatively tiny polder, Stage IV may be passed over.

3. DEVELOPMENT OF BREACH IN STAGES I, II AND III

Figure 2 shows the flow through the initial breach at $t = t_0^+$ shortly after the start of the breaching process at $t = t_0$. From a hydraulic point of view the slopes of dikes are very steep, i.e. $\sin\beta >> C_f$ (the slope angle β is defined here as the inclination of the inner slope of the dike in the breach in the flow direction with respect to a horizontal line, C_f is the bottom friction coefficient). This means that the water depth at the top of the inner slope at $x = 0$ (x is the coordinate along the inner slope) is equal to the critical depth d_c. The flow on the inner slope accelerates between $x = 0$ and $x = l_n$, and is virtually uniform for $x \geq l_n$. Consequently the capacity to transport sand also increases between $x = 0$ and $x = l_n$ and is nearly constant for $x \geq l_n$. This means that the rate of erosion increases along the stretch $0 < x < l_n$ and is nearly constant for $l_n \leq x \leq l_a$ (where l_a is the adaptation length of the suspended

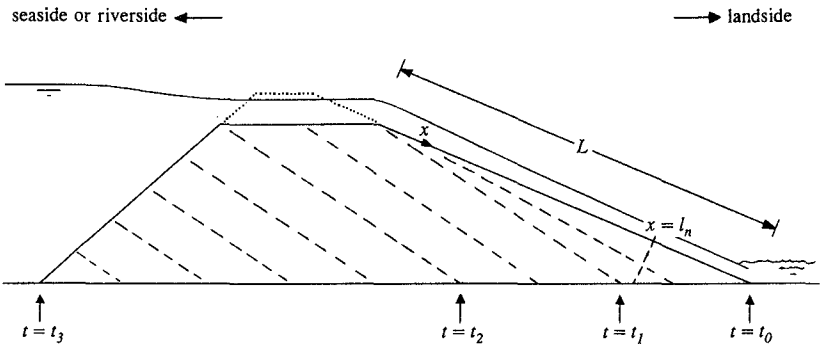

Figure 2 Flow over dike in the breach at $t = t_0^+$ shortly after the start of the breaching process (solid line) and development of inner slope of dike in the breach in Stages I, II and III (dashed lines).

sediment transport, similarly to l_n being the adaptation length of the flow). As a result of this the inner slope becomes steeper and steeper along the slope and in time along the stretch $0 < x < l_n$, and for $l_n \leq x \leq l_a$ the inclination of the inner slope remains constant. The slope angle along $0 < x < l_n$ will, however, not exceed a limit β_1 (say $\beta_1 \approx \phi$, where ϕ is the angle of internal friction). If this limit has been reached along the entire stretch $0 < x < l_n$ (at $t = t_1$), the rate of erosion becomes constant for $0 \leq x < l_n$ as indicated by the lines for $t \geq t_1$ in Figure 2, and Stage II starts.

In Stage II retrograde of the inner slope of the dike in the breach occurs at constant angle β_1, resulting in a decrease of the width of the dike-crest in the breach. Stage II ends when the width of the dike-crest has become zero (at $t = t_2$).

It can be concluded that for $t_0 < t \leq t_2$ the rate of erosion of the inner slope in the breach is controlled by the erosion at $x = l_n$ (or also the erosion along the stretch $l_n \leq x \leq l_a$). This means that only the rate of erosion at $x = l_n$ has to be known.

In Stage I the width of the channel (initial breach) in the crown of the dike remains at its initial value. The increase of the depth of the channel in the inner slope causes also an increase of the width of this channel in the slope (see Figure 1). At $t = t_1$ the width of the breach starts to grow at the downstream side of the dike-crown.

As long as the flow accelerates, its capacity to transport sediment increases. This means that the adaptation length for the sediment transport is always larger than the adaptation length for the flow, i.e. $l_a > l_n$. Visser (1998) has derived the following practical approximation for l_n:

$$\frac{l_n}{L} \approx 10 \frac{h}{H_D} \tag{1}$$

where h is the depth of the breach in the crest of the dike, H_D is the height of the dike above the polder level and L is the length of the inner slope.

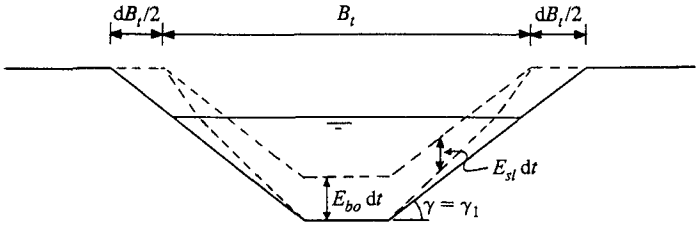

Figure 3 Increase dB_t in time dt of breach width B_t near the inflow in Stage III.

A relatively high dike in The Netherlands has a height $H_D \approx 10\,\text{m}$. If it is assumed that $h \approx 1\,\text{m}$ (i.e. the 1 m thick clay-layer at the crest of the dike has been washed out by the high water), then the ratio $l_n/L \approx 1$. Hence, the development of the inner slope in Stages I and II of the breach erosion process of such a typical dike will be as shown in Figure 2 for $x \leq l_n$.

Figure 2 shows also the triangular cross-section of the dike through the axis of the breach at $t = t_2$. Due to the proceeding erosion process, the top of the dike in the breach starts to drop. As a result, both the discharge per unit width q_{br} and the breach width increase in Stage III. It is assumed that also in this stage the angle of the inner slope remains at the critical value β_1. So again the rate of erosion is constant along the entire stretch $0 \leq x \leq l_n$, and also in the interval $t_2 < t < t_3$ it is entirely determined by the erosion at the toe of the slope.

At $t = t_2$ the width of the breach at the upstream side of the crown also starts to grow (see Figure 1). The rate of erosion at the breach bottom (E_{bo}) is larger than the erosion rate at the side-slopes (E_{sl}) due to the larger flow velocities (as a result of the larger water depths). For the same reason the erosion rate at the toe of the side-slopes is larger than higher on the slopes. This means that in Stage III the side-slope erosion is entirely controlled by the erosion at the bottom (i.e. the increase of the breach depth). Hence, the rate of increase of breach width is controlled by the rate of erosion at the breach bottom (see Figure 3):

$$\frac{dB_t}{dt} = \frac{2}{\tan\gamma_1} E_{bo} \tag{2}$$

In Stage III the breach growth accelerates drastically when deepening of the breach opening magnifies the inflow rate and the latter accelerates the erosion process. Consequently the flow and the sand transport through the breach change drastically in this stage: from a supercritical flow with a Froude number Fr much larger than 1 at $t = t_2$ to a supercritical flow with Fr slightly above 1 at $t = t_3$, from sheet flow transport with a Shields' mobility parameter θ of orders 10 and 100 at $t = t_2$ to sediment transport with θ of order 1 at $t = t_3$ (see Visser, 1998).

It is clear that the duration of the breach erosion process in Stages I, II and III depends largely on the dimensions of the initial breach. The larger these are, the shorter the total duration of these stages is, and consequently an accurate description of the breach erosion process in Stages I, II and III is then less important for the evaluation of the rate of flooding of the protected low-lying land.

4. BREACH DEVELOPMENT IN STAGES IV AND V

The continuation of the breach erosion process after the complete wash-out of the dike in the breach at t_3 depends on the following geometrical and material conditions of the dike:

- the resistance against further erosion of the base of the dike;
- the presence or absence of a berm and a toe construction on the outer slope and its ability to protect the outer slope against further erosion;
- the presence or absence of a relatively high foreland and its resistance against erosion.

Three types of breaches can be distinguished, dependent of these conditions. In a Type A breach the vertical erosion at the breach inflow is prevented by a solid clay foundation of the dike, or by a solid berm and a solid toe construction on the outer slope or by a solid, relatively high foreland (solid means here: with relatively high resistance against erosion). Dikes breach as Types B or C in the absence of a solid clay foundation, or a solid berm and a solid toe construction or a solid high foreland. If a relatively high (erodible) foreland is present then the dike breaches as Type B, otherwise as Type C. The Types A, B and C breaches are described further in next.

Type A breach

If the base of the dike consists of a solid clay-layer, then this layer will considerably slow down or prevent further vertical erosion, see Figure 4. This means that the breach continues to grow laterally in Stages IV and V, as shown in Figure 5. Since the erosion at the toe of the side-slopes is larger than higher on the slopes, the angle γ remains at its critical value γ_1. Hence, the erosion at the toe of each of the side-slopes (E_{sl} in Figure 5) determines the erosion of the overall side-slope, and consequently also the growth of the breach width. The discharge through the breach can be described simply by the formula for the flow over a broad-crested weir.

The lower parts of the outer slopes of sea dikes and river dikes in The Netherlands are protected against waves and currents by a (low water) berm and a toe construction. Less is known about the behaviour of these constructions in breaching dikes. It is, however, likely that these constructions may hinder or slow down further growth of the scour hole in upstream direction in cases where the foundation of the dike does not consist of solid clay. Downstream of the low water berm the breach continues to grow in vertical direction resulting in the formation of a scour hole, see Figure 9. The berm acts as a spillway (broad-crested or sharp-crested, which has only a secondary influence on the discharge coefficient of the spillway) controlling the breach inflow rate. Then the growth of the breach width is also determined at this upstream control section, resulting in an increase of the breach width as in the above situation of a solid base of the dike.

In cases where the dike has a relatively high foreland with a relatively large resistance against erosion, the development of the breach inflow and the breach growth is similar to that of a dike with a solid low water berm on the outer slope.

Types B and C breaches

If the base of the dike does not have much resistant against erosion and the dike does not have a solid berm and a solid toe construction on the outer slope, the breach continues to grow vertically (scour hole grows both with and against the flow, see Figures 9 and 11) and laterally (widening of the breach, see Figures 10 and 12).

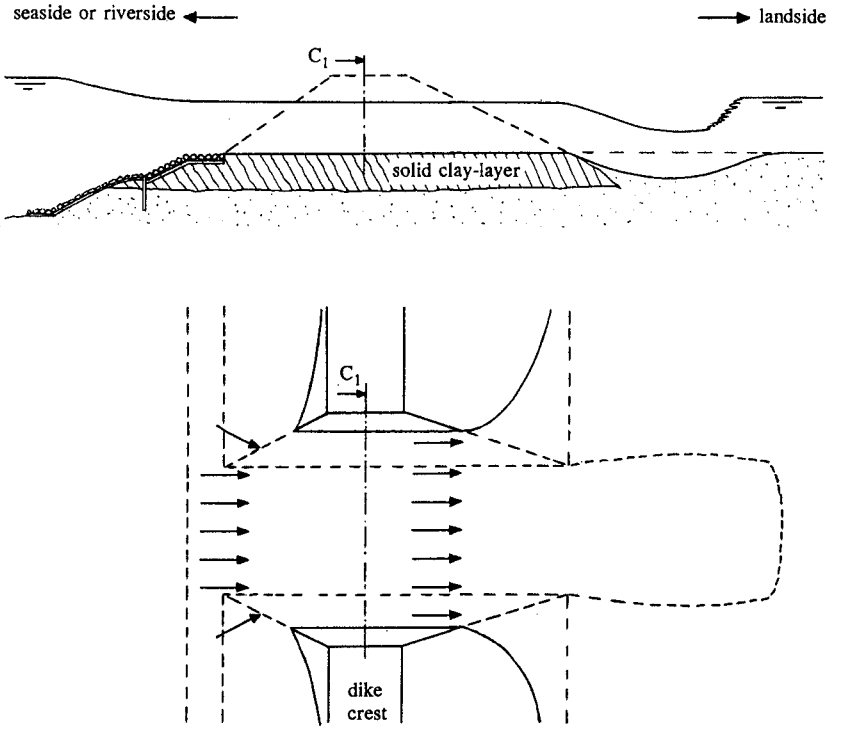

Figure 4 Cross-section and top view of flow in Stage IV through a breach in a dike constructed on a solid clay-layer (Type A breach).

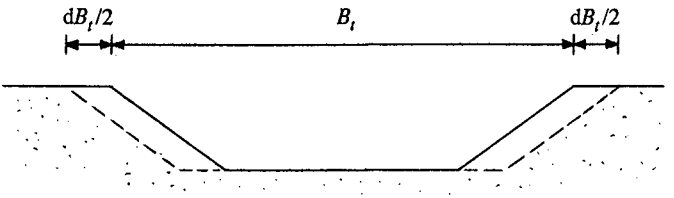

Figure 5 Cross-section C_1 (see Figure 4) of breach showing increase of breach width B_t in a Type A breach in Stages IV and V.

Upstream of the breach a spillway is formed which controls the breach inflow. The alignment of this spillway depends on the height of the foreland in front of the dike. The alignment of the overfall will be curved (elliptic or circular) in a Type B breach

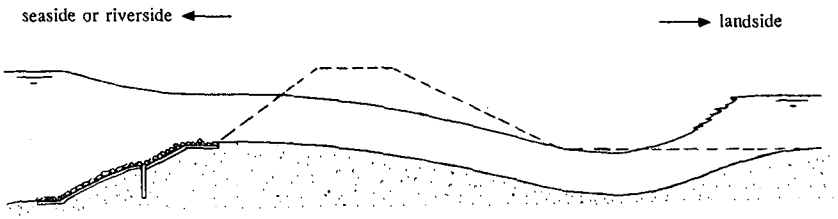

Figure 6 Flow in Stage IV through a breach when a toe construction protects the lower part of the outer slope against further erosion.

in a dike with a relatively high foreland (see Figure 7). In a situation where the outer slope abuts on the water course the shape of the spillway will be straight in the middle and curved near the side-slopes; this is called a Type C breach (see Figure 8).

As described in Chapter 3, the growth of the breach width in Stage III is controlled by the rate of erosion at the breach bottom (E_{bo}), and not by the erosion at the side-slopes (E_{sl}). In Stages IV and V, however, it is the erosion rate at the side-slopes (E_{sl}) that determines the increase of the breach width (see Figures 5, 8 and 10):

$$\frac{dB_t}{dt} = \frac{2}{\tan\gamma_1} E_{sl} \tag{3.3}$$

The argument behind this conclusion is simple. The order of magnitude of the widths of final-breaches is 100 m (see Visser, 1998), while the order of magnitude of their depths is 10 m. Hence, the widths of final breaches have always been much larger then their depths, so that:

$$E_{bo} << \frac{2}{\tan\gamma_1} E_{sl} \tag{3.4}$$

Visser (1998) argues that the side-slope erosion in Stages IV and V is governed by the flow at the upstream spillway, which simplifies the modelling of the breach growth process significantly.

In Stage V ($t_4 < t \leq t_5$) the breach continues to grow laterally. The continuous flow through the breach causes the water level in the polder to increase and the flow velocity in the breach to decrease, resulting in a deceleration of the breach growth.

At t_5 the flow velocities in the breach become so small (incipient motion) that the breach erosion stops. As far as the rate of flooding of the polder is concerned, Stages IV and V are the most important stages, since in these stages most of the water is discharged through the breach and the ultimate dimensions of the breach are determined.

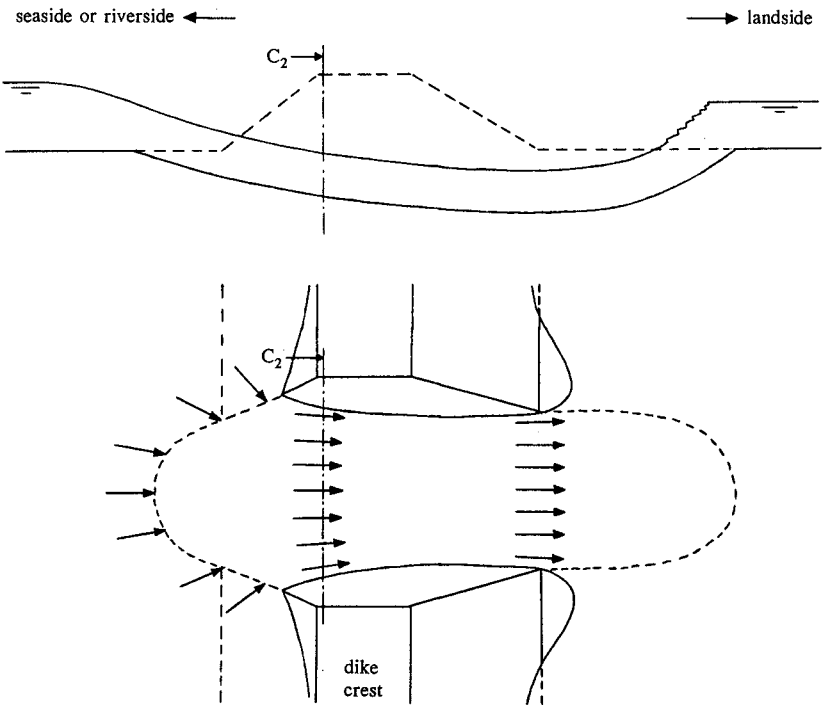

Figure 7 Cross-section and top view of flow in a Type B breach in Stage IV.

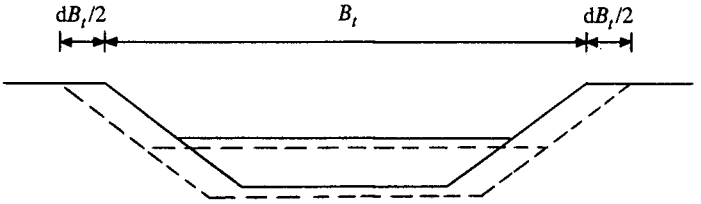

Figure 8 Cross-section C_2 (see Figure 7) showing growth of breach width B_t in a Type B breach in Stages IV and V.

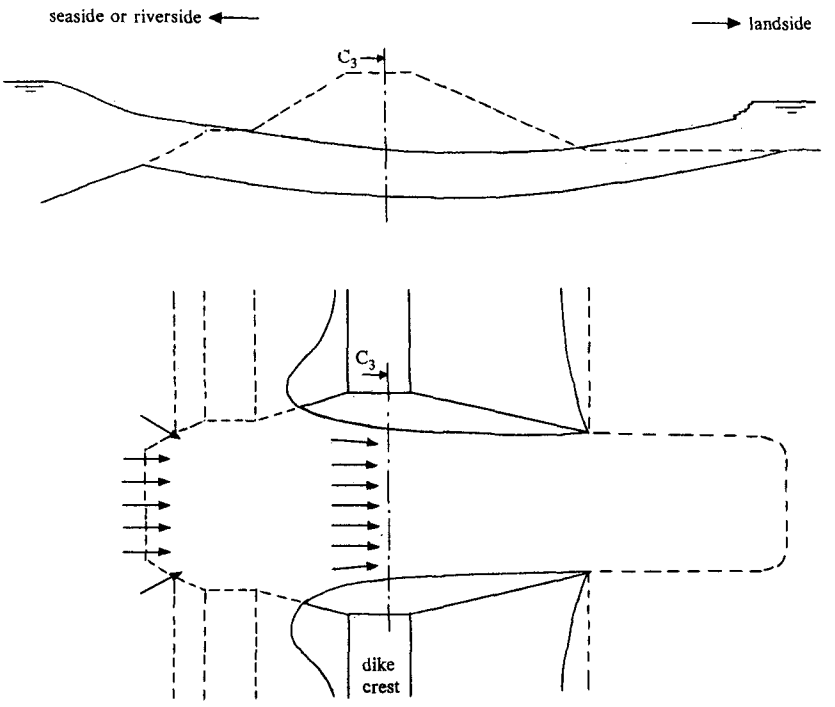

Figure 9 Cross-section and top view of flow in a Type C breach in Stage IV.

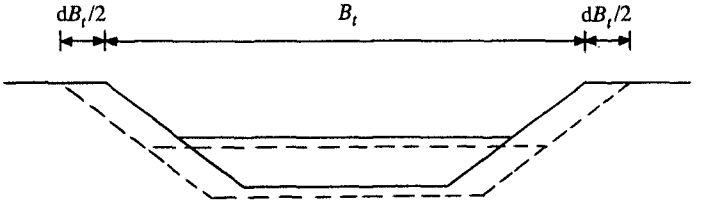

Figure 10 Cross-section C_3 (see Figure 9) showing growth of breach width B_t in a Type C breach in Stages IV and V.

5. MATHEMATICAL MODEL

Based on the five-step breach erosion process described above, a mathematical model for the growth of a breach in a sand-dike and the inflow rate through the breach has been developed. It is assumed that the dike was constructed with sand and that the clay-layers on the slopes do not decelerate the erosion process.

An essential part of a breach erosion model is the description of the entrainment of the sediment and its transport through the breach. In the mathematical model a simplified version of Galappatti's (1983) description for the entrainment of sediment is applied. This approach requires, however, a formulation for the equilibrium value of the sediment transport. None of the existing sediment transport formulae has been derived and tested for the relatively steep slopes in the initial stages and the large flow velocities throughout most of the breach erosion process. For application into the model, a number of existing sediment transport formulae has been tested to breach erosion tests (see Visser, 1995b), leaving only a few formulae with a reasonable performance. These transport formulae have been implemented into the model for the confrontation with experimental results and prototype data.

The numerical version of the model (BRES) has been written in C^{++} for use on a personal computer.

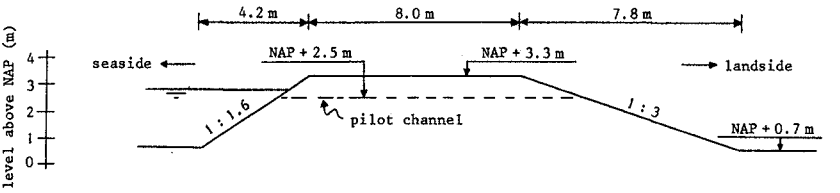

Figure 11 Cross-section of sand-dam in Zwin'94 experiment (NAP is reference level in The Netherlands at about mean sea level).

6. ZWIN'94 FIELD EXPERIMENT

The Zwin'94 experiment was performed in the Zwin Channel, a tidal inlet at the Dutch-Belgian border connecting the nature-reserve The Zwin with the North Sea (see Visser et al., 1996). The Zwin area measures about 1.5 km^2; the mean tidal prism is about 350000 m^3. The experiment was done in quiet autumn weather, with negligible wave heights against the sand-dam.

A sand-dam closing of the Zwin Channel (see Figure 11) was built with a height $H_D = 2.6$ m above the channel bottom, a width at the crest of 8 m and a length of about 200 m. The inclination of the outer slope was 1 : 1.6, that of the inner slope 1 : 3. A small trapezoidal pilot channel, 0.8 m deep and with a width of about 1 m at the breach bottom and about 3.6 m at the dike crest was made in the upper part of the dam to ensure breaching near the middle of the Zwin Channel.

The experiment started at $t = t_0 = 0$, about 20 minutes before high water, with the flow of water through the pilot channel. At 3 locations upstream and 3 locations

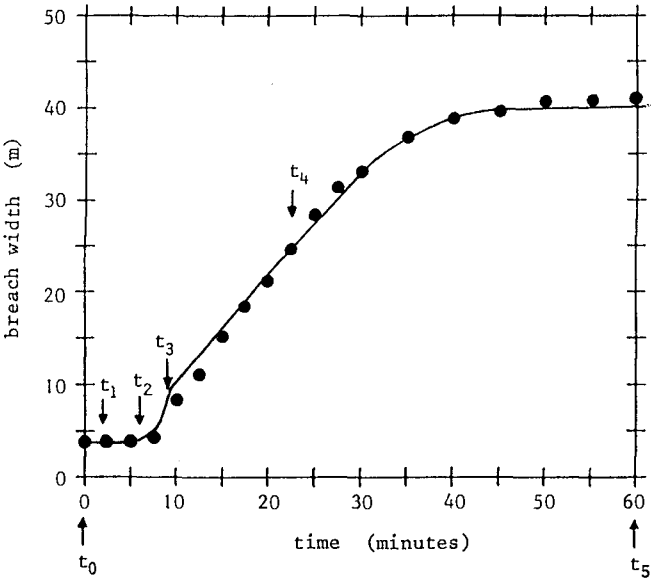

Figure 12 Comparison of model prediction (solid line) for width of the breach at the dike top (B_t) and observed B_t in Zwin'94 experiment (dotted line).

downstream from the breach, current velocity meters (Ott propeller type) and pressure probes measured continuously horizontal flow velocities and water elevations, respectively. The breach erosion process was both video-taped and photographed (marks put in the dike-top allowed the observation of the dimensions of the breach at different times from the video-images, slides and photos). A total number of 40 vibration probes, buried in the sandy bottom of the Zwin Channel, detected the development of the breach under water in Stages IV and V. Each probe acted as a burglar-alarm: by measuring its own rate of vibration it could detect when the erosion process had exposed it to the flowing water. The vibration probe system was tested and calibrated in a laboratory flume. The signals of all vibration probes were recorded on the hard disks of several personal computers. At $t = t_5 \approx 60$ min the flow velocities in the breach had become so small that the erosion process stopped. The Zwin'94 field experiment has clearly confirmed the five-step breach erosion mechanism as described above and shown in Figure 1. Figure 12 shows the result of the observations of the growth of the breach width B_t in time (observed at the top of the dike): B_t increased from $B \approx 3.6$ m at $t = t_0 = 0$ up to $B_t \approx 41$ m at $t = t_5 \approx 60$ min.

The data set of the Zwin'94 experiment is very useful for the validation of mathematical breach erosion models. Reference is made to Visser et al. (1996) and Visser (1998) for details about the data set resulting from this experiment.

7. COMPARISON OF MODEL PREDICTION WITH FIELD DATA

Figure 12 shows the comparison of the model prediction with the data of the Zwin' 94 experiment. It can be concluded that the agreement of the model prediction with the experimental data is good. This result has been obtained applying the Bagnold-Visser formula (see Visser, 1989) in Stages I, II and III and Van Rijn's (1984a,b) sand transport formulation in Stages IV and V.

Visser (1998) has applied the model also to a laboratory experiment and to a prototype dike failure of the 1953 flood in The Netherlands. For descriptions of both cases and details of these validations of the model reference is made to Visser (1998).

REFERENCES

Bagnold, R.A., 1963. Mechanics of marine sedimentation. In *'The Sea: Ideas and Observations', 3*, Interscience, New York, USA, pp. 507-528.

Galappatti, R., 1983. A depth-integrated model for suspended transport. *Comm. on Hydraulics, Rep. 83-7*, Dept. Civil Eng., Delft Univ. Techn., Delft, The Netherlands.

Kraak, A.W., Bakker, W.T, Graaff, J. van de, Steetzel, H.J. and Visser, P.J., 1995. Breach-growth research programme and its place in damage assessment for a polder. *Proc. 24th Int. Conf. Coastal Eng.*, Kobe, Japan, 1994, pp. 2197-2206.

Van Rijn, L.C., 1984a. Sediment transport. Part I: bed load transport. *J. Hydr. Eng., 110*, pp. 1431-1456.

Van Rijn, L.C., 1984b. Sediment transport. Part II: suspended load transport. *J. Hydr. Eng., 110*, pp. 1613-1641.

Visser, P.J., 1989. A model for breach growth in a dike-burst. *Proc. 21st Int. Conf. Coastal Eng.*, Malaga, Spain, pp. 1897-1910.

Visser, P.J., 1995a. A model for breach growth in sand-dikes. *Proc. 24th Int. Conf. Coastal Eng.*, Kobe, Japan, 1994, pp. 2755-2769.

Visser, P.J., 1995b. Application of sediment transport formulae for sand-dike breach erosion. *Comm. on Hydraulic and Geotechnical Eng., Rep. no. 94-7*, Dep. Civil Eng., Delft Univ. of Technology, Delft, The Netherlands.

Visser, P.J., 1998. Breach growth in sand-dikes. *Ph.D. thesis*, Fac. Civil Eng., Delft Univ. Techn., Delft, The Netherlands.

Visser, P.J., Kraak, A.W., Bakker, W.T, Steetzel, Smit, M.J., Snip, D.W., H.J. and Graaff, J. van de, 1996. A large-scale experiment on breaching in sand-dikes. *Proc. Coastal Dynamics'95*, Gdansk, Poland, 1995, pp. 583-594.